

ALGORITHM FOR COMPUTING \underline{S} PARAMETERS AND THEIR USE FOR STUDYING EFFICIENCY OF ELECTROMAGNETIC ENERGY WIRELESS TRANSFER SYSTEMS

MARILENA STĂNCULESCU, MIHAI IORDACHE, DRAGOȘ NICULAE, LAVINIA BOBARU, VICTOR BUCATĂ

Key words: Wireless power transfer systems (WPTS), \underline{S} parameters, Efficiency.

In this paper we present the suitable formulation of \underline{S} parameters using the electric circuit theory along with their practical use to improve the efficiency of the wireless power transfer systems (WPTS). We also present an algorithm used for computing \underline{S} parameters. In order to compute the parameters \underline{S} , for different structures of WPTS, we may use either the modified nodal equations, generated by circuit symbolic analysis program (CSAP), either the state equations, generated by symbolic state equation generation (SYSEG). Based on analog circuits theory in harmonic state in complex domain, the accuracy for defining parameters \underline{S} is confirmed, comparing our results with the ones obtained using the advanced design system (ADS) software with specific routines.

1. INTRODUCTION

In order to describe linear devices in harmonic state at low and medium frequencies, one may use: impedance parameters Z , admittance parameters Y , hybrid parameters H , and transfer parameters T [1–9].

For higher frequencies, these parameters can no longer be used since their measurements require special arrangements. For instance, to compute impedance parameters of a two-port network (2PN), the output port must be short-circuited, which makes impossible the measurement at higher frequencies. In this case, the equipment is not able to measure the actual voltage and the actual current at the 2PN's gates. Moreover, many active devices cannot operate by a stable manner when short-circuits or open-circuits occur. The quantities that should be used at these frequencies are the transverse waves. [4].

The scattering parameters (\underline{S}) – are complex quantities, device dependant and they can be computed or measured for any equipment which posses or not electromagnetic field propagation phenomena. If propagation phenomena are present, their significance is connected to the port to port electromagnetic field reflection [5]. If no propagation, then the term power wave is used because their dependence is connected to the active power absorbed by the load function of its working frequency. Following this, in circuit theory, where there is no propagation as in waveguides, the scattering parameters have been introduced [6].

The various possibilities to introduce these parameters, present in literature [7–9] can make difficult their understanding and can raise problems in interpreting their physical significance. The carefully approach in studying these parameters is greatly advised. For example, a paper that offers conversion formulae between these parameters [10] is under critic in another [11].

A correct formulation that will have as a consequence the understanding of scattering parameters is important for high frequency applications which include active and passive components in integrated circuits and especially for (WPTS) [12].

In this paper we present the suitable formulation of \underline{S} parameters using the electric circuit theory and their practical use to improve the efficiency of the wireless power transfer

systems. We also present an algorithm used for computing \underline{S} parameters.

The computation procedures use advanced computation software and routines, such as ADS [13], Ansoft Extractor Q3D [14], Feko [15] etc.

2. \underline{S} PARAMETERS DEFINITION

\underline{S} – the scattering parameters – are used to compute the power transmission efficiency in microwave networks and in wireless power transfer [16, 17]. There are efficient techniques to measure \underline{S} parameters, such as using a vector network analyzer (VNA). For this reason, these parameters are suited for improving the efficiency of the electromagnetic energy transmission processes [18–24].

To correctly define the scattering parameters \underline{S} for a two-port network (2PN), let us consider the circuits given in Fig. 1.

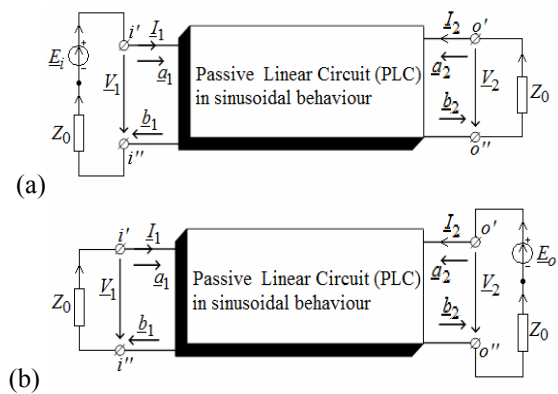


Fig. 1 – Passive linear circuit tin sinusoidal behaviour:
a) the circuit used to define the parameters \underline{S}_{11} and \underline{S}_{21} ;
b) the circuit used to define the parameters \underline{S}_{12} \underline{S}_{22} .

As a first step, we want to change the pairs of variables (V_1, I_1) and (V_2, I_2) with the pairs (a_1, b_1) and, respectively (a_2, b_2) , in the equations bellow:

$$\begin{aligned} V_1 &= \sqrt{Z_0}(a_1 + b_1); \quad I_1 = \frac{1}{\sqrt{Z_0}}(a_1 - b_1) \\ V_2 &= \sqrt{Z_0}(a_2 + b_2); \quad I_2 = \frac{1}{\sqrt{Z_0}}(a_2 - b_2) \end{aligned} \quad (1)$$

where Z_0 is a real positive variable, called *reference (characteristic) impedance*.

By similarity with the wave equation, the solution a_1 (a_2) represents the incident wave from the gate $i' - i''$ ($o' - o''$) as in Fig. 1, and b_1 (b_2) is the reflected wave from the same gate.

For linear circuits, the variables associated with each gate can be considered as a superposition of incident (direct) waves and of reflected (indirect) waves [9, 20].

The modules of the new variables have the units of \sqrt{AV} , which shows that the squares of these modules have the dimensions of an electric power.

Usually, the reference impedance is equal to the module of the load impedance. From relation (1) it results:

$$\begin{aligned} a_1 + b_1 &= \frac{1}{\sqrt{Z_0}} V_1, \quad a_1 - b_1 = \sqrt{Z_0} I_1 \\ a_2 + b_2 &= \frac{1}{\sqrt{Z_0}} V_2, \quad a_2 - b_2 = \sqrt{Z_0} I_2 \end{aligned} \quad (2)$$

and then, by solving with respect to the new variables, we obtain:

$$\begin{aligned} a_1 &= \frac{1}{2} \left(\frac{1}{\sqrt{Z_0}} V_1 + \sqrt{Z_0} I_1 \right) = \frac{1}{2\sqrt{Z_0}} (V_1 + Z_0 I_1) \\ b_1 &= \frac{1}{2} \left(\frac{1}{\sqrt{Z_0}} V_1 - \sqrt{Z_0} I_1 \right) = \frac{1}{2\sqrt{Z_0}} (V_1 - Z_0 I_1) \end{aligned} \quad (3)$$

respectively,

$$\begin{aligned} a_2 &= \frac{1}{2} \left(\frac{1}{\sqrt{Z_0}} V_2 + \sqrt{Z_0} I_2 \right) = \frac{1}{2\sqrt{Z_0}} (V_2 + Z_0 I_2) \\ b_2 &= \frac{1}{2} \left(\frac{1}{\sqrt{Z_0}} V_2 - \sqrt{Z_0} I_2 \right) = \frac{1}{2\sqrt{Z_0}} (V_2 - Z_0 I_2). \end{aligned} \quad (4)$$

The scattering parameters \underline{S} of a 2PN (Figs. 1, a and b) satisfy the following equations between the incident and the reflected signals:

$$\begin{aligned} b_1 &= \underline{S}_{11} a_1 + \underline{S}_{12} a_2 \\ b_2 &= \underline{S}_{21} a_1 + \underline{S}_{22} a_2 \end{aligned} \quad (5)$$

where: \underline{S} parameters for the 2PN in Fig. 1 have the following meanings: \underline{S}_{11} , (\underline{S}_{22}) – is the reflection coefficient from gate 1 (gate 2); \underline{S}_{21} (\underline{S}_{12}) – is the transmission coefficients from gate 1 to gate 2 (gate 2 to gate 1).

The parameters \underline{S}_{11} and \underline{S}_{21} , associated to a linear 2PN (Fig. 1 a), are defined as follows:

- **Parameter \underline{S}_{11}**

$$\begin{aligned} \underline{S}_{11} &= \left. \frac{b_1}{a_1} \right|_{a_2=0 \Leftrightarrow V_2=-Z_0 I_2, \underline{Z}_1=Z_0, V_1=E_i-Z_0 I_1} = \\ &= \left. \frac{V_1 - Z_0 I_1}{V_1 + Z_0 I_1} \right|_{a_2=0 \Leftrightarrow V_2=-Z_0 I_2, \underline{Z}_1=Z_0, V_1=E_i-Z_0 I_1} = \\ &= \frac{E_i - 2Z_0 I_0}{E_i} = 1 - 2\underline{A}_{1i}, \end{aligned} \quad (6)$$

where $\underline{A}_{1i} = \left. \frac{Z_0 I_1}{E_i} \right|_{V_2=-Z_0 I_2, \underline{Z}_1=Z_0}$ is the voltage transfer

factor (amplification), computed when at port $i' - i''$, we have connected the *emf* E_i in series with the input impedance $Z_i = Z_0$, and at the output port ($o' - o''$) we have connected the impedance $Z_o = Z_l = Z_0$;

- **Parameter \underline{S}_{12}**

$$\begin{aligned} \underline{S}_{12} &= \left. \frac{b_1}{a_2} \right|_{a_1=0 \Leftrightarrow V_1=-Z_0 I_1, \underline{Z}_1=Z_0, \underline{Z}_l=Z_0} = \\ &= \left. \frac{V_1 - Z_0 I_1}{V_2 + Z_0 I_2} \right|_{a_1=0 \Leftrightarrow V_1=-Z_0 I_1, \underline{Z}_1=Z_0, \underline{Z}_l=Z_0} =, \\ &= \frac{-2Z_0 I_1}{E_o} = -2\underline{A}_{io} \end{aligned} \quad (7)$$

where $\underline{A}_{io} = \left. \frac{Z_0 I_1}{E_o} \right|_{V_1=-Z_0 I_1, \underline{Z}_1=Z_0}$ is the voltage transfer

(amplification) factor, when the characteristic impedance Z_0 is connected to the input port $i' - i''$ (E_i being zero) and at the output port ($o' - o''$) we have connected the impedance $Z_l = Z_0$ in series with t.e.m. E_e ;

The parameters \underline{S}_{21} and \underline{S}_{22} , associated to a 2PN (Fig. 1 b), are defined as follows:

- **Parameter \underline{S}_{21}**

$$\begin{aligned} \underline{S}_{21} &= \left. \frac{b_2}{a_1} \right|_{a_2=0 \Leftrightarrow V_2=-Z_0 I_2, \underline{Z}_1=Z_0, \underline{Z}_l=Z_0, V_1=E_i-Z_0 I_1} = \\ &= \left. \frac{V_2 - Z_0 I_2}{V_1 + Z_0 I_1} \right|_{a_2=0 \Leftrightarrow V_2=-Z_0 I_2, \underline{Z}_1=Z_0, \underline{Z}_l=Z_0, V_1=E_i-Z_0 I_1} = \\ &= \frac{-2Z_0 I_2}{E_i} = -2\underline{A}_{oi}, \end{aligned} \quad (8)$$

where $\underline{A}_{oi} = \left. \frac{Z_0 I_2}{E_i} \right|_{V_2=-Z_0 I_2, \underline{Z}_1=Z_0, \underline{Z}_l=Z_0}$ is the voltage

amplification factor from input to output, in the conditions mentioned in relation (8);

- **Parameter \underline{S}_{22}**

$$\begin{aligned} \underline{S}_{22} &= \left. \frac{b_2}{a_2} \right|_{a_1=0 \Leftrightarrow V_1=-Z_0 I_1, \underline{Z}_1=Z_0, \underline{Z}_l=Z_0, V_2=E_o-Z_0 I_2} = \\ &= \left. \frac{V_2 - Z_0 I_2}{V_2 + Z_0 I_2} \right|_{a_1=0 \Leftrightarrow V_1=-Z_0 I_1, \underline{Z}_1=Z_0, \underline{Z}_l=Z_0, V_2=E_o-Z_0 I_2} = \\ &= \frac{E_o - 2Z_0 I_2}{E_o} = 1 - 2\underline{A}_{2o}, \end{aligned} \quad (9)$$

where $\underline{A}_{2o} = \left. \frac{Z_0 I_2}{E_o} \right|_{V_1=-Z_0 I_1, \underline{Z}_1=Z_0}$ is the voltage

amplification factor when at the input port $i' - i''$ we have

connected the characteristic impedance Z_0 (E_i being zero) and at the output port ($o' - o''$) we have connected the impedance $Z_1 = Z_0$ in series with the emf E_o . The reflection factor S_{11} and the transmission factor S_{21} can be measured with the VNA.

The \underline{S} parameters generation for analog linear circuits and for nonlinear analog circuits, (piecewise linear around the operating point) in precise polarization conditions of the electronic devices, can take place only by small signals simulations [11, 12].

The linear circuit obtained may be analyzed as a multi-port network. Each gate is sequentially excited by small signals and the response is measured and transformed in \underline{S} parameters.

Figures 1 a and b offer the representation of a wave in a 2PN. For each port the following quantities are being defined: [4–7, 9, 11]:

- a_1 – input signal at gate 1; b_1 – output signal at gate 1;
- a_2 – input signal at gate 2; b_2 – output signal at gate 2.

\underline{S} – parameters are defined function of a characteristic impedance, which is, in general, 50Ω .

To generate S parameters for nonlinear circuits, we use the program large-signal S -parameter simulation (LSSP) [14], which uses the harmonic balance method. The simulation based on harmonic balance is a high-level signal simulation containing also the effects due to the electronic components nonlinearity. S parameters both at small signals and high-level signals are defined as ratios between the incident and the reflected waves.

3. \underline{S} PARAMETER COMPUTATION – ALGORITHM DESCRIPTION

To compute the parameters S , for different structures of a wireless power transfer system (WPTS), we may use either the modified nodal equations, generated by circuit symbolic analysis program (CSAP), either the state equations, generated by symbolic state equation generation (SYSEG) [10–12].

As it follows, we present the computation algorithm for S parameters computation for a series-series connection of the resonator, when we used CSAP program for generating the modified nodal equations (the results are identical to the one obtained using SYSEG program).

We also used CSAP program for the other three connections of the magnetically coupled resonators: series-parallel, parallel-series and parallel-parallel (same results with those by SYSEG), the computation algorithms of S parameters are similar with the computation algorithm for series-series connection [10–12, 19]. The validation of the results obtained with CSAP and SYSEG took place by comparing these results with the one obtained with the program ADS [13].

The algorithm for \underline{S} parameters computation for series series magnetically coupled resonators (SSMCR):

Step_1. Computation of the \underline{S}_{11_ss} and \underline{S}_{21_ss} parameters. We consider the SSMCR as presented in Fig. 2.

To compute the parameters according to (6) and according to (8), the analysis of the circuit from Fig. 2 is performed in harmonic regime, with the program CSAP [11], with condition $R_i = R_L = Z_0$. We kept R_i and R_L for computing the active power transmission efficiency

$$\eta_{21_ss} = 100 \cdot P_{RL_ss} / P_{1_ss} \quad \text{where} \quad P_{RL_ss} = R_L \cdot I_{RL_ss}^2, \\ P_{1_ss} = \text{Re}(E_i \cdot I_{i_ss}^*).$$

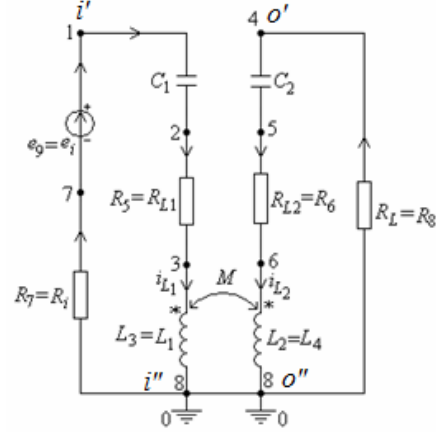


Fig. 2 – The magnetic circuit used to generate \underline{S}_{11_ss} and \underline{S}_{21_ss} .

After running the program, CSAP outputs two files. One contains full symbolic modified nodal equations (the electric potentials of the $n-1$ independent nodes of the analyzed circuit and the currents corresponding to the branches incompatible with the modified nodal method (MNM), and the other contains the full symbolic expressions of the branch currents and voltages.

Step_2. Computation of the efficiencies $\eta_{21_f_ss}$ for the following numerical values of the parameters: $C_1=0.188\text{e-}06$ F; $C_2=0.4\text{e-}06$ F; $L_1=50.0\text{e-}06$ H; $L_2=24.0\text{e-}06$ H; $M=8.4896\text{e-}06$ H; $R_{L1}=0.0162 \Omega$; $R_{L2}=0.011 \Omega$; $R_i=1.5 \Omega$; $R_L=6.0 \Omega$; $R_c=6.0 \Omega$; $E_i=100.0$ V.

The expression of the efficiency $\eta_{21_f_ss}$ is:

$$\eta_{21_f_ss} = -3.1916950\text{e-}13 \cdot f^4 / (-4496.6970 - .96433133\text{e-}15 \cdot f^4 + .23797344\text{e-}5 \cdot f^2). \quad (10)$$

Step_3. Computation of the factor \underline{S}_{11_ss} , which, for $R_c = 6 \Omega$ and the numerical values of these parameters, presented above, have the expression (according to the definition):

$$\underline{S}_{11_f_ss} := .40000000\text{e-}1 \cdot (-.32132751\text{e-}3 \cdot f^2 - .14614945\text{e-}8 \cdot j \cdot f^3 + 500000. + 4.0174592 \cdot j \cdot f + .65964050\text{e-}13 \cdot f^4) / (-.17131636\text{e-}4 \cdot f^2 - .16573989\text{e-}9 \cdot j \cdot f^3 + 20000. + .44405197 \cdot j \cdot f + .26385618\text{e-}14 \cdot f^4). \quad (11)$$

Step_4. Computation of \underline{S}_{21_ss} parameter. \underline{S}_{21_ss} parameter is the most important \underline{S} coefficient because $\text{abs}(\underline{S}_{21})^2$ represents the efficiency of the signal transmission for SSMCR from the input to the output and it is computed with the relation:

$$\underline{S}_{21_f_ss} = -2.0 \cdot (R_c \cdot I_{RL_f_ss}) / E_i. \quad (12)$$

For $R_c = 6 \Omega$ and for the numerical values of the parameters presented above, the parameter $\underline{S}_{21_f_ss}$ has the expression [17, 18]:

$$\underline{S}_{21_f_ss} = -3.7948556\text{e-}10 \cdot f^3 \cdot (.44405197 \cdot f - .16573989\text{e-}9 \cdot f^3 - .17131636\text{e-}4 \cdot j \cdot f^2 + 20000. \cdot j + .26385618\text{e-}14 \cdot j \cdot f^4) / (-.62936049\text{e-}19 \cdot f^6 + .40000000\text{e9} + .25184115\text{e-}9 \cdot f^4 - .48808326 \cdot f^2 + .69620088\text{e-}29 \cdot f^8), \quad (13)$$

and the signal transmission efficiency from input to output $\eta_{21_S21_f_ss}$ is, according to [17, 18]:

$$\begin{aligned} \text{eta}_{21_S21_f_ss} = & .90005806e10 \cdot f^6 \cdot (- \\ & .12202082e44 \cdot f^2 + .62960294e34 \cdot f^4 - \\ & .15734012e25 \cdot f^6 + \\ & .10000000e53 + .17405021e15 \cdot f^8) / (- \\ & .78670061e17 \cdot f^6 + .50000000e45 + .31480144e27 \cdot \\ & f^4 - .61010408e36 \cdot f^2 + 8702511 \cdot f^8)^2. \end{aligned} \quad (14)$$

The variation with frequency of the modules of the parameters $\underline{S}_{11_f_ss}$ and $\underline{S}_{21_f_ss}$ are presented in Fig. 4a, where they are computed using the programs CSAP [11] and SYSEG [11] and, respectively, in Fig. 4b, where they are computed using ADS.

The graphs of the efficiencies $\text{eta}_{21_f_ss}$ and $\text{eta}_{21_S21_f_ss}$ function of frequency f are given in Fig. 5a, where they are computed using CSAP and SYSEG and, respectively in Fig. 5b, where they are computed using ADS.

From Figs. 4a, b and 5a, b we conclude that the variations function of frequency of the quantities computed using the programs ADS, SYSEG and ADS are identical, which confirms the validity of the used computation formulas.

Step_5. Computation of the coefficients \underline{S} . To determine these scattering factors, the resonator is powered at gate $o' - o''$ and R_c is connected at the input gate (in general $Z_0 = Z_c$).

Step_6. Computation of the efficiency corresponding to the active power transfer from the output gate $o' - o''$ to the input gate $i' - i''$, for the following numerical values provided at step 2.

$\text{eta}_{12_f_ss}$ has the expression:

$$\begin{aligned} \text{eta}_{12_f_ss} = & .37502416e-14 \cdot f^4 / \\ & / (37930.276 + .52508180e-14 \cdot f^4 - .28001551e-4 \cdot f^2). \end{aligned} \quad (15)$$

Step_7. Computation of parameter \underline{S}_{22} . First we compute using CSAP the voltage transfer factor \underline{A}_{2o} , and then the parameter \underline{S}_{22_ss} has, according to the definition (9), the expression:

$$\begin{aligned} \underline{S}_{22_f_ss} = & .40000000e-1 \cdot (- .32123498e-3 \\ & \cdot f^2 + .14440086e-8 \cdot j \cdot f^3 + 500000. - \\ & 3.9707010 \cdot j \cdot f + .65964050e-13 \cdot f^4) / (- .17131636e-4 \\ & \cdot f^2 - .16573989e-9 \\ & \cdot j \cdot f^3 + 20000. + .44405197 \cdot j \cdot f + .26385618e-14 \cdot f^4). \end{aligned} \quad (16)$$

Step_8. Computation of parameter $\underline{S}_{12} = -2.0 \cdot \underline{A}_{io} = -2.0 \cdot R_c \cdot \underline{I}_{1_f_ss} / \underline{E}_o$. Parameter \underline{S}_{12_ss} is very important, because the efficiency of power transfer from the output gate $o' - o''$ to the input gate $i' - i''$ has the expression $\text{eta}_{12_S12_ss} = 100.0 \cdot \text{abs}(\underline{S}_{12})^2$.

For $R_c = 6\Omega$ and for the numerical values presented above, $\underline{S}_{12_f_ss}$ has the expression:

$$\begin{aligned} \underline{S}_{12_f_ss} = & -.18974277e-14 \cdot j \cdot f^3 / (- .85658178e-9 \cdot f^2 - \\ & .82869945e-14 \cdot j \cdot f^3 + 1. + .22202598e-4 \\ & \cdot j \cdot f + .13192810e-18 \cdot f^4), \end{aligned} \quad (17)$$

and the efficiency of transmitting the signals from output to input $\text{eta}_{12_S12_f_ss}$ is given by the relation:

$$\begin{aligned} \text{eta}_{12_S12_f_ss} = & .36002319e21 \cdot f^6 / (.62960293e32 \cdot f^4 - \\ & .12202082e42 \cdot f^2 - .15734014e23 \cdot f^6 + .10000000e51 \\ & + .17405024e13 \cdot f^8). \end{aligned} \quad (18)$$

The dependencies on frequency of the modules of parameters $\underline{S}_{22_f_ss}$ and $\underline{S}_{12_f_ss}$ are presented in Fig. 6a, where they are computed using CSAP and SYSEG and, respectively in Fig. 6b, where they are computed using ADS. The plot of efficiencies $\text{eta}_{12_f_ss}$ and $\text{eta}_{12_S12_f_ss}$ depending on frequency f are given in Fig. 7 a, where they are computed using CSAP and SYSEG and, respectively in Fig. 7b, where they are computed using ADS.

From Figs. 6a, b and 7a, b, we notice the frequency variations of the quantities computed using the programs CSAP, SYSEG and ADS are identical, which confirm the validity of the used computation formula.

The plots of efficiencies $\text{eta}_{12_f_ss}$ and $\text{eta}_{12_S12_f_ss}$ vs. frequency are presented in Fig. 9a, where they are computed using CSAP and SYSEG and, respectively in Fig. 9b, where they are computed using ADS.

Figures 8a, b and 7a, b shows the variations with frequency of the quantities computed using CSAP, SYSEG and ADS are identical, which confirms the validity of the used computation formula.

It can be easily proved that between the matrices \underline{Z} , \underline{T} , \underline{Y} and \underline{S} there are the following relations:

$$\underline{Z} = (\underline{I}_2 - \underline{S})^{-1} \cdot (\underline{I}_2 + \underline{S}) \underline{Z}_0, \quad (19)$$

where \underline{I}_2 is the order 2 unit matrix;

$$\underline{S} = (\underline{Z} - \underline{Z}_0 \underline{I}_2) \cdot (\underline{Z} + \underline{Z}_0 \underline{I}_2)^{-1} \quad (20)$$

$$\underline{T} = \frac{1}{\underline{Z}_{21}} \begin{bmatrix} \underline{Z}_{11} & \underline{Z}_{11} \cdot \underline{Z}_{22} - \underline{Z}_{12} \cdot \underline{Z}_{21} \\ 1 & \underline{Z}_{22} \end{bmatrix}; \quad (21)$$

$$\underline{Z} = \frac{1}{\underline{C}} \begin{bmatrix} \underline{A} & \underline{A} \cdot \underline{D} - \underline{B} \cdot \underline{C} \\ 1 & \underline{D} \end{bmatrix}. \quad (22)$$

$$\underline{Y} = \frac{1}{\underline{Z}_{11} \underline{Z}_{22} - \underline{Z}_{12} \underline{Z}_{21}} \begin{bmatrix} \underline{Z}_{22} & -\underline{Z}_{12} \\ -\underline{Z}_{21} & \underline{Z}_{11} \end{bmatrix}. \quad (23)$$

To define the input and output complex impedances and the reflection coefficients, the system consisting of two magnetically coupled coils, used in WPTS, is equivalent with the passive linear 2PN (in harmonic state) presented in Fig. 3 [1, 10, 12].

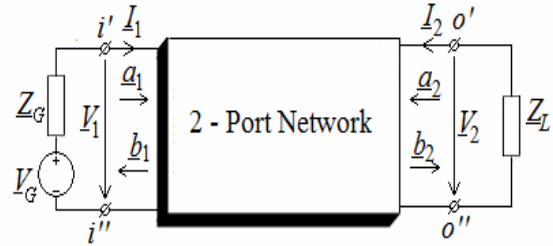


Fig. 3 – Passive linear 2PN connected to generator and load.

The active power, received at the input terminals $i' - i''$, by the 2PN from Fig. 3, has the expression [1, 20]:

$$P_1 = P_{in} = \text{Re}(\underline{V}_1 \cdot \underline{I}_1^*) = |\underline{a}_1|^2 - |\underline{b}_1|^2. \quad (24)$$

In equation (24), we considered relations (2) and that the complex representation of a sinusoidal quantity $x(t) = \sqrt{2} X \sin(\omega t + \alpha_x)$ is $\underline{X} = X e^{j\alpha_x}$.

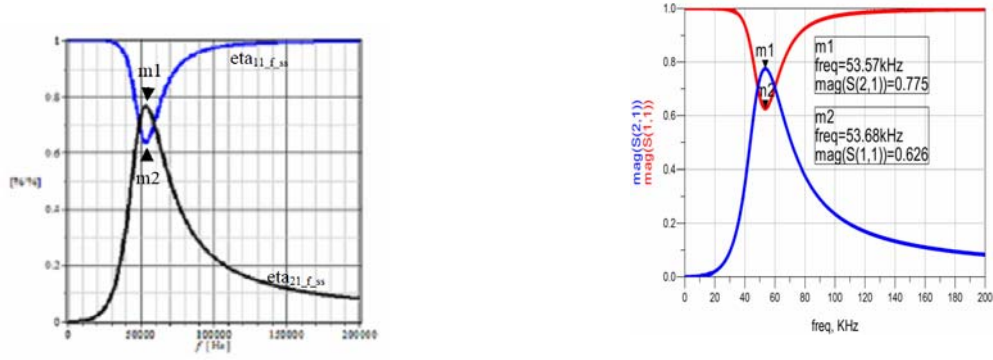
The active power given at the output terminals $o' - o''$, by the 2PN from Fig. 3, has the expression:

$$P_2 = P_L = -\text{Re}(\underline{V}_2 \cdot \underline{I}_2^*) = -|\underline{a}_2|^2 + |\underline{b}_2|^2. \quad (25)$$

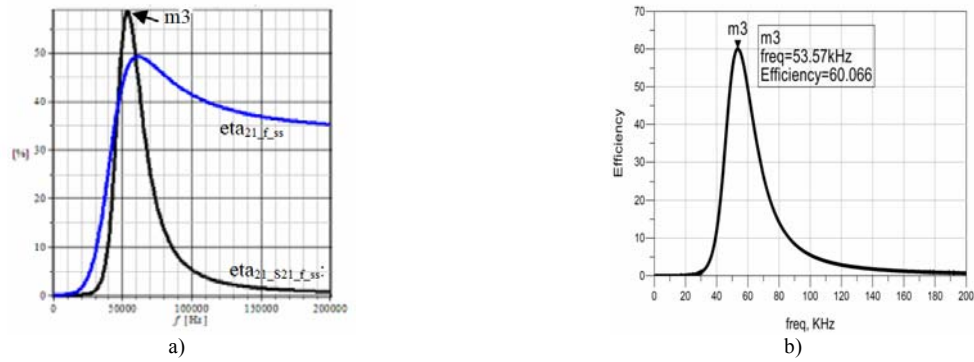
The power losses are given by the difference between P_1 and P_2 :

$$\begin{aligned} P_{loss} = & P_1 - P_2 = |\underline{a}_1|^2 + |\underline{a}_2|^2 - |\underline{b}_1|^2 - |\underline{b}_2|^2 = \\ = & (\underline{a}^*)^t \cdot \underline{a} - (\underline{b}^*)^t \cdot \underline{b} \end{aligned} \quad (26)$$

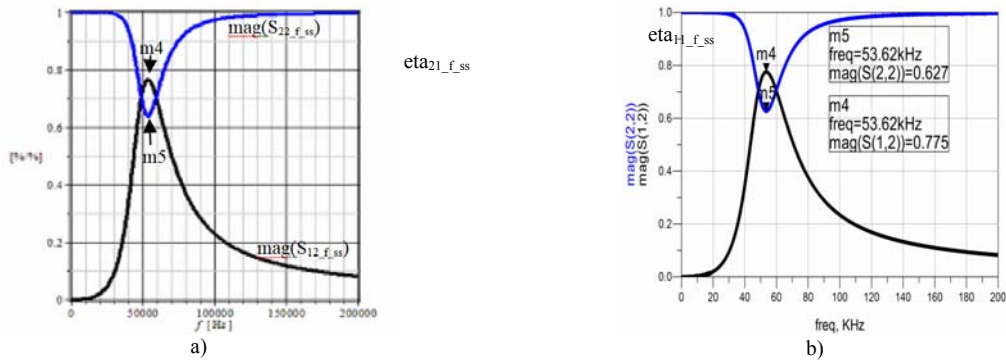
where $\underline{a} = \begin{bmatrix} \underline{a}_1 \\ \underline{a}_2 \end{bmatrix}$ and $\underline{b} = \begin{bmatrix} \underline{b}_1 \\ \underline{b}_2 \end{bmatrix}$.



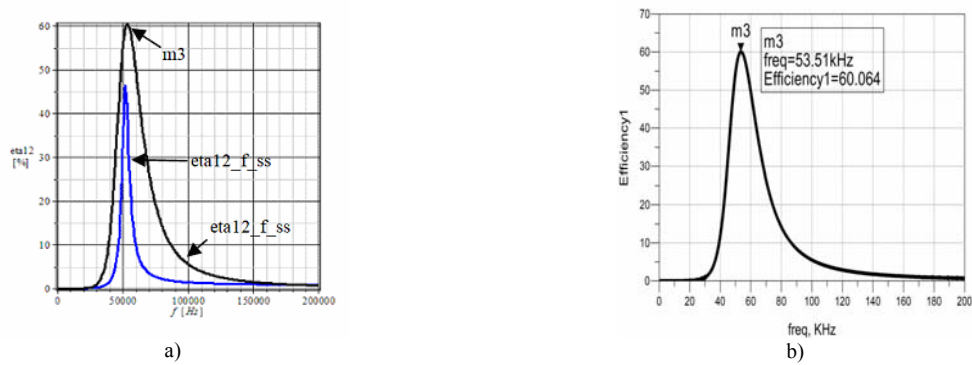
a) b)
Fig. 4 – Frequency variations of efficiencies $\eta_{21_f_ss}$ and $\eta_{21_S21_f_ss}$:
a) computed using CSAP and SYSEG; b) computed using ADS.



a) b)
Fig. 5 – Frequency variations of efficiencies $\eta_{21_f_ss}$ and $\eta_{21_S21_f_ss}$:
a) computed using CSAP and SYSEG; b) computed with ADS.



a) b)
Fig. 6 – Frequency variations of modules $S_{22_f_ss}$ and $S_{12_f_ss}$:
a) computed using CSAP and SYSEG; b) computed with ADS.



a) b)
Fig. 7 – Variations with frequency of $\eta_{12_f_ss}$ and $\eta_{12_S12_f_ss}$:
a) computed using CSAP and SYSEG; b) computed using ADS.

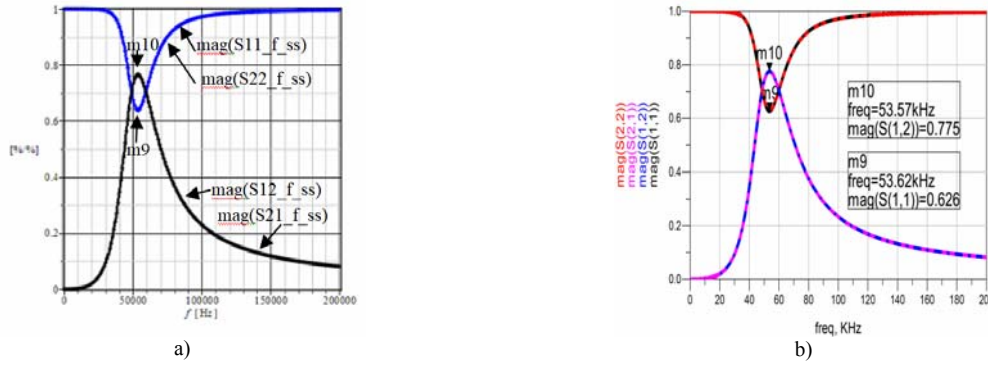


Fig. 8 – Frequency variations of the modules of parameters $S_{11_f_ss}$, $S_{21_f_ss}$, $S_{22_f_ss}$ and $S_{12_f_ss}$:
a) computed using CSAP and SYSEG; b) computed using ADS.

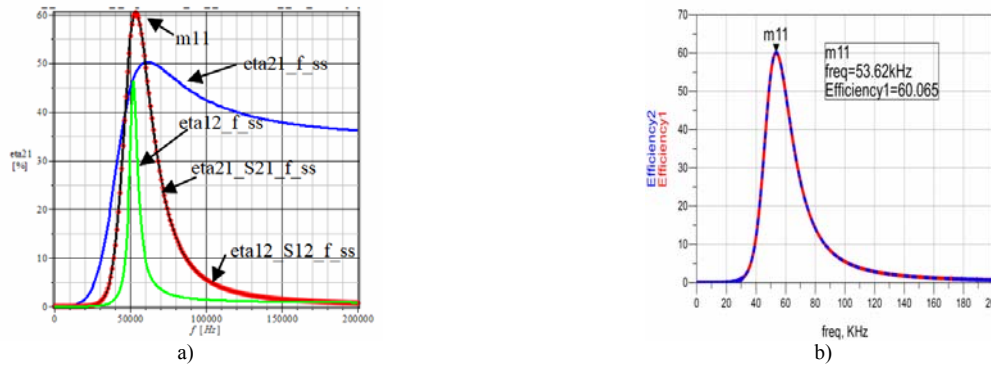


Fig. 9 – Frequency variations of efficiencies $\eta_{21_f_ss}$, $\eta_{21_S21_f_ss}$, $\eta_{12_f_ss}$ and $\eta_{12_S12_f_ss}$:
a) computed using CSAP and SYSEG; b) computed using ADS.

4. CONCLUSIONS

The correct definition, based on electric circuit theory of the \underline{S} parameters, allowed their automatic generation, using the state equations or the modified nodal equations. Once \underline{S} parameters have been generated, for a set of frequencies, the following can be computed: the matrices \underline{T} , \underline{Z} and \underline{Y} ; the reflection coefficients; the active power transmission efficiencies; the signal transmission efficiencies; the input and output impedances; Thévenin equivalent generator.

Considering the two resonators, used in the WPTS, as a linear 2PN in harmonic state, we computed, as a function of \underline{S} parameters all the above-mentioned parameters. In this paper we presented the practical use of these parameters to make the electromagnetic power transfer more efficient. By comparing the variations with frequency of the active power transmission efficiencies η_{21} and η_{12} with those corresponding to the signals transmission η_{21_S21} and η_{12_S12} we notice that the frequencies corresponding to extreme points are identical. The curves corresponding to the frequency variations of the active power transmission efficiencies have only one maximum at different frequencies, while the variations with frequency curves are identical. The linear passive 2PN which is equivalent with the system consisting of the two magnetically coupled coils allows the computation of the maximum active power transmitted to the load.

We conclude that the variation obtained using CSAP, SYSEG and ADS are completely identical, which confirms the validity of the used computation formulae. The

accuracy of defining the scattering parameters \underline{S} , based on analog circuits theory in harmonic state in complex domain, (6) – (9), is confirmed by the results obtained using the dedicate software ADS which has specific routines for computing \underline{S} parameters.

Received on March 16, 2018

REFERENCES

1. Marilena Stănculescu, M. Iordache, D. Niculae, Lavinia Iordache, V. Bucată, S. Parameter Computation and Their Use for Electromagnetic Energy Wireless Transmission, IJCT – International Journal of Computers & Technologies, **12**, pp. 7097–7108, 2016.
2. L. Mandache, A. Marinescu, M. Iordache, On feasibility and optimization of WiTricity technology for implantable medical devices, 2016 ISFEE, Bucharest, pp. 1–6, 2016.
3. A. Marinescu, M. Tarata, M. Iordache, Current State of WiTricity Technology Application Perspectives for Implantable Medical Devices, Bulletin of Micro and Nanoelectrotechnologies, **VII**, 3–4, pp. 45–50 (2015).
4. S.J. Orfanidis, *Electromagnetic Waves and Antennas*, 2008, <http://eceweb1.rutgers.edu/~orfanidi/ewa/>.
5. Gabriela Ciuprina, Aurel Sorin Lup, Alina Tomescu, Parametrii S în aplicații de înaltă frecvență, SNET'12 Conference Proceedings, 14.12.2012, Politehnica University of Bucharest.
6. R.B. Marks, D.F. Williams, A general waveguide circuit theory, Journal of Research of the National Institute of Standards and Technology, **97**, 1992, pp. 533–562.
7. George Lojewski, *Dispozitive și circuite de microunde*, Editura Tehnică, Bucharest, 2005.
8. S.J. Orfanidis, *Electromagnetic Waves and Antennas*, 2008, Disponibilă online la <http://www.ece.rutgers.edu/~orfanidi/ewa/>.
9. Anca Tomescu, F.M.G. Tomescu, *Sisteme cu microunde*, MatrixROM, Bucharest, 2001.
10. D.A. Frickey, Conversions between S, Z, Y, H, ABCD, and T parameters which are valid for complex source and load impedances, IEEE Trans. on Microwave Theory and Techniques, **42**, pp. 205–211, 1994.

11. R.B. Marks and D.F. Williams, *Comments on conversions between S , Z , Y , H , $ABCD$, and T parameters which are valid for complex source and load impedances*, IEEE Trans. on Microwave Theory and Techniques, **43**, pp. 914–915, 1995.
12. T. Imura, H. Okabe, Y. Hori, *Basic Experimental Study on Helical Antennas of Wireless Power Transfer for Electric Vehicles by using Magnetic Resonant Couplings*, Proc. of Vehicle Power and Propulsion Conf., Sept. 2009, IEEE Xplore, 978-1-4244-2601-4/010/2010, pp. 936–940.
13. Advanced Design System (ADS), <http://www.keysight.com/en/pc-1297113/advanced-design-system-ads?cc=US&lc=eng>.
14. ANSOFT Q3D EXTRACTOR, User Guide, www.ANSOFT.com.
15. FEKO - EM Simulation Software, <https://www.feko.info/support>.
16. M. Iordache, Lucia Dumitriu, D. Niculae, Georgiana Zainea, *Power Transfer by Magnetic Induction Studied by Coupled Mode Theory*, Book chapter in the book, *Wireless Power Transfer*, Editor J.I. Agbinya, River Publishers Series in Communications, Denmark, 2015, Second Edition, pp. 1–69.
17. M. Iordache, *Symbolic, Numeric – Symbolic and Numeric Simulation of Analog Circuits – User Guides*, Edit. Matrix Rom, Bucharest, 2015.
18. M. Iordache, Lucia Dumitriu, *Computer-Aided Simulation of Analogue Circuits – Algorithms and Computational Techniques*, Vol. I + II, Politehnica Press, Bucharest 2014.
19. Agilent Technologies, AGILENT TECHNOLOGIES, *Large-Signal S-Parameter Simulation*, Sept, 2004.
20. W. Chen, R.A. Chinga, S. Yoshida, J. Lin, C. Chen, and W. Lo, *A 25.6 W 13.56 MHz wireless power transfer system with a 94% efficiency GaN class-E power amplifier*, Microwave Symposium Digest, IEEE MTT-S International, August 2012, pp. 1–3.
21. W. C. Brown, *The history of wireless power transmission*, Solar Energy, **56**, 1, pp. 3–21 (1996).
22. A. Kurs et al., *Wireless Power Transfer via Strongly Coupled Magnetic Resonances*, MIT, 2007 Science, **317**, 5834, pp. 83–86, 2007.
23. S.R. Pennock, P.R. Shepherd, *Microwave Engineering with Wireless Applications*, McGraw-Hill Profesional © 1998.
24. A.K. Sah, and D.P. Pant, *Analysis and Optimization of Wireless Power Transfer Link*, Proc. of Int. Conf. on Techn. & Innovation Mang. and IOE Graduate Conf., Oct. 10–11, 2014, pp. 82–93.